RESEARCH ARTICLE

Katharine V. Cashman · Ross C. Kerr ·
Ross W. Griffiths

A laboratory model of surface crust formation and disruption on lava flows through non-uniform channels

Abstract Crust formation on basaltic lava flows dictates conditions of both flow cooling and emplacement. For this reason, flow histories are dramatically different depending on whether lava is transported through enclosed lava tubes or through open channels. Recent analog experiments in straight uniform channels (Griffiths et al. J Fluid Mech 496:33–62, 2003) have demonstrated that *tube flow*, dictated by a stationary surface crust, can be distinguished from a *mobile crust regime*, where a central solid crust is separated from channel walls by crust-free shear zones, by a simple dimensionless parameter ϑ, such that $\vartheta < 25$ produces tube flow and $\vartheta > 25$ describes the mobile crust regime. ϑ combines a previously determined parameter ψ, which describes the balance between the formation rate of surface solid and the shear strain that disrupts the solid crust, with the effects of thermal convection (described by the Rayleigh number Ra).

Here we explore ways in which ϑ can be used to describe the behavior of basaltic lava channels. To do this we have extended the experimental approach to examine the effects of channel irregularities (expansions, contractions, sinuosity, and bottom roughness) on crust formation and disruption. We find that such changes affect local flow behavior and can thus change channel values of ϑ. For example, gradual widening of a channel results in a decrease in flow velocity that causes a decrease in ϑ and may allow a downflow transition from the mobile crust to the tube regime. In contrast, narrowing of the channel causes an increase in flow velocity (increasing ϑ), thus inhibiting tube formation.

We also quantify the fraction of surface covered by crust in the mobile crust regime. In shallow channels, variations in crust width (d_c) with channel width (W) are predicted to follow $d_c \sim W^{5/3}$. Analysis of channelized lava flows in Hawaii shows crustal coverage consistent with this theoretical result along gradually widening or narrowing channel reaches. An additional control on crustal coverage in both laboratory and basaltic flows is disruption of surface crust because of flow acceleration through constrictions, around bends, and over breaks in slope. Crustal breakage increases local rates of cooling and may cause local blockage of the channel, if crusts rotate and jam in narrow channel reaches. Together these observations illustrate the importance of both flow conditions and channel geometry on surface crust development and thus, by extension, on rates and mechanisms of flow cooling. Moreover, we note that this type of analysis could be easily extended through combined use of FLIR and LiDAR imaging to measure crustal coverage and channel geometry directly.

Keywords Surface crust · Lava flows · Solidification · Channel flow · Irregularities

K. V. Cashman (✉)
Department of Geological Sciences, University of Oregon,
Eugene, OR 97403-1272, USA
e-mail: cashman@uoregon.edu
Tel.: +1-541-346-4323
Fax: +1-541-346-4692

R. C. Kerr · R. W. Griffiths
Research School of Earth Sciences, Australian National
University,
Canberra, ACT 0200, Australia

Introduction

Hawaiian lava flows are classified as pāhoehoe, 'a'ā, or block lava on the basis of their surface morphology (Dutton 1884; Macdonald 1953). Morphological distinctions reflect differences in flow emplacement dynamics, particularly in the structure of lava feeder systems. Lava transport in pāhoehoe flow fields is commonly through robust and well-insulated lava tubes (e.g., Hon et al. 1994; Peterson et al. 1994), whereas 'a'ā flows are fed by large channels only partially covered by (semi-)solid surface crusts (Fig. 1; e.g., Lipman and Banks 1987). As the surface coverage of incandescent lava controls the rate of heat loss from the flow surface (Crisp and Baloga 1990, 1994) and consequent rate of crystallization (Cashman et al. 1999), thermal (and rheological) histories are very different for lava transport systems with or without continuous surface crusts.

Fig. 1 Photograph of braided lava channels, Episode 5, Pu`u `O`o eruption, Kīlauea Volcano, Hawaii, 1983. Note the braided nature of the lava channels, the variability of surface crustal coverage, the presence of crust-free shear zones along some channel reaches, and short crust-free sections of the channels that probably reflect flow over local breaks in slope. USGS photograph by J. Griggs

Flow conditions that stabilize or disrupt solidified crust are poorly constrained, particularly for the large, open-channel flows (e.g., Kauahikaua et al. 2003). On the one hand, limiting conditions necessary to produce tube or open-channel flow may be addressed through consideration of crust stability, treated as a balance between crust strength and applied stress (Kilburn 2004). However, implementation of this approach requires that relationships between the dynamics of flow and crust development be fully understood. Dynamical aspects of flow are important not only from consideration of heat transport mechanisms but also for conditions that may generate the mechanical stress necessary for crustal disruption. A complementary approach is suggested by a recent laboratory analog study of flow through straight uniform channels (Griffiths et al. 2003), which parameterizes the transition from open-channel to tube flow through consideration of the relative rates of flow advection and flow cooling, together with the effects of thermal convection. Here we assess the applicability of this latter approach to basaltic lava flows, extend existing experiments to examine the effects of channel geometry on crust formation, and use our results to evaluate changes in crustal coverage of two lava channels from Kīlauea Volcano, Hawai'i.

Background

In Hawaii, the style of lava flow emplacement (through enclosed tubes or through open channels) is controlled by a combination of flow duration and the time-dependent history of the effusion rate supplying the flow. Long-lived basaltic eruptions, often with low average effusion rates ($<\sim$5–10 m^3 s^{-1}), typically produce complex flow fields fed primarily by lava tubes (Rowland and Walker 1990). Lava tubes form more readily when lava supply is steady for extended periods of time (weeks to months) and when

slopes and/or effusion rates are low (Guest et al. 1987; Holcomb 1987; Peterson et al. 1994; Hon et al. 1994, 2003; Calvari and Pinkerton 1998, 1999; Kauahikaua et al. 1998, 2003). Tube formation permits thermally efficient transport of lava over long distances. For example, Hawaiian lava tubes typically have cooling rates of 0.6–1°C km^{-1} (Cashman et al. 1994; Helz et al. 1995, 2003) and average flow velocities of 1.5–3 m s^{-1} (Peterson et al. 1994; Kauahikaua et al. 1998), yielding cooling rates of $\sim$3$\times$10^{-3}°C s^{-1}. In contrast, open-channel flows are typically short-lived (days to weeks) and produced by eruptions of moderate to high effusion rates ($>$10 m^3 s^{-1}; Rowland and Walker 1990), although when the effusion is unsteady, short-lived channels may form at lower rates of flow (Cashman et al. 1999; Hon et al. 2003). Lava cools rapidly down the channel (5–10°C km^{-1}), resulting in cooling rates an order of magnitude higher than those measured during lava transport in tubes (Fig. 2).

Syn-emplacement cooling and crystallization of lava flows has important implications for conditions of lava transport. The initial advance of basaltic lava flows is controlled primarily by effusion rate (Pinkerton and Wilson 1994; Kilburn 2000; Kauahikaua et al. 2003), consistent with fluid dynamical models that track flow of Newtonian or Bingham fluids through uniform channels (e.g., Hulme 1974; Dragoni and Tallarico 1994; Tallarico and Dragoni 1999, 2000; Sakimoto and Gregg 2001). However, continued flow of lava through established channels is strongly controlled by conditions of cooling. Simple parameterizations assume that flow should cease when the crust becomes sufficiently thick (strong) to prevent further forward motion. Cooling-based flow models include (1) Pinkerton and Wilson's (1994) use of the Graetz number Gr ($=Ud_e^2/\kappa L$, where U is the mean flow velocity, d_e the equivalent diameter of the flow, κ is the thermal diffusivity of the lava, and L is the flow length) to predict final flow lengths and (2) Kilburn's (2004)
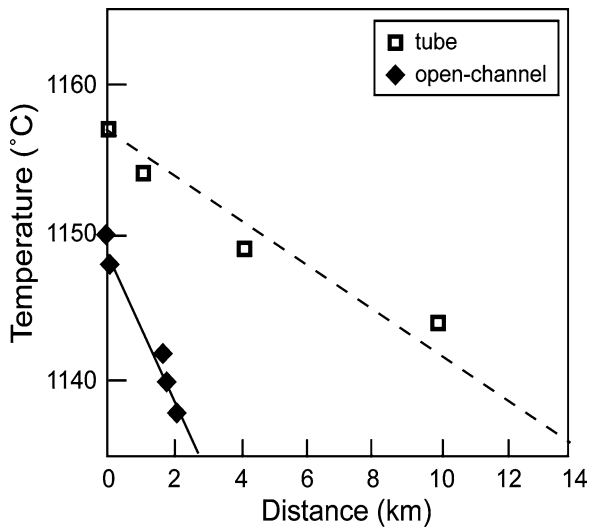
Fig. 2 Down-flow cooling rates for tube-fed (pāhoehoe) and open-channel ('a'ā) flows in Hawaii. Lava flow rate is similar for both data sets (~3 m³ s⁻¹). Data from Cashman et al. (1994, 1999)

application of a failure criterion for solid crusts. Critical for models of crust development, however, is a complete understanding of how channelized lava cools. Thermal models of flow emplacement (e.g., Crisp and Baloga 1990, 1994; Hon et al. 1994; Keszthelyi 1995; Keszthelyi and Denlinger 1996; Neri 1998; Sakimoto and Zuber 1998; Kerr 2001) show that rapid, radiative cooling dominates when incandescent lava is exposed at the surface. The relative magnitude of radiative cooling is commonly described by an empirical determination of the fraction of the flow surface (f) that exposes incandescent lava (Crisp and Baloga 1990, 1994), with flow cooling being most efficient under conditions that minimize crustal coverage (large f).

Still lacking are models that fully link the thermal and rheological evolution of the lava to the flow dynamics (e.g., Pinkerton and Wilson 1994; Kilburn 1996; Harris and Rowland 2001). Existing numerical models rely on simple parameterizations and require extensive calibration with active flows (e.g., Harris and Rowland 2001; Crisci et al. 2004). A key unknown in such models, and one that is controlled by poorly understood mechanisms, is the evolution of the solidified flow surface. FLOWGO (Harris and Rowland 2001), the only model to include crustal coverage of the flow surface, uses an empirical function for the fractional crust coverage of the flow surface ($f_{crust} = 1 - f$) based on local flow velocity (U) in the channel: $f_{crust} = 0.9 \exp(-0.16U)$. This formulation assumes that f_{crust} never exceeds 0.9 (i.e., there is no possibility of lava tube formation) and predicts that most of the variation in f_{crust} will occur for flow velocities of 1–10 m s⁻¹ (over which f_{crust} varies from 0.77 to 0.18). Here we take a somewhat different approach and use analog models and parameterization of flow and cooling conditions to constrain crustal coverage of lava channels. Together the models and parameterizations allow us to address (1) transitions between open-channel and tube flow regimes, (2) the combined roles of flow and cooling on the development of surface crust (f_{crust}), and (3) the effect of channel irreg-

ularities (sinuosity, width changes and bottom roughness) on crustal coverage.

Analog models

The mechanisms at work in coupling cooling, solidification, and flow, can be examined using analog experiments. The most commonly used laboratory analog for lava is polyethylene glycol (PEG), a wax that is liquid at room temperature but solidifies at about 19°C (cf. Griffiths 2000). PEG experiments by Fink and Griffiths (1990, 1992) and Griffiths and Fink (1993) have shown that the surface morphology of axisymmetric and two-dimensional flows can be characterized by a single dimensionless parameter

$$\psi = \frac{U_0 t_s}{H_0}, \tag{1}$$

where t_s is the time to cool the flow surface to the solidification temperature and U_0 and H_0 are velocity and depth scales for viscous gravitational spreading of an isothermal fluid. The parameter ψ is thus a measure of the solidification time relative to the advection time H_0/U_0 expected without solidification (Griffiths and Fink 1993 ; Griffiths 2000). For subaerial basaltic lava flows, solidification times do not vary extensively and ψ may thus be related directly to effusion rate. High effusion rates produce large values of ψ, meaning that cooling times are long relative to timescales of flow, and thus cooling does little to modify flow conditions. In contrast, low effusion rates lead to small ψ, a condition where cooling dominates. Although ψ was originally defined for solidification of viscous fluid, a similar parameter ψ_B applies when the extruded fluid has a yield strength and is undergoing slow plastic deformation (Griffiths and Fink 1997). Slope affects flow behavior by shifting the values of ψ or ψ_B appropriate for transitions between different flow regimes (Gregg and Fink 2000; Lyman et al. 2004).

Experiments in straight uniform channels

In channelized lava flows, surface crusts are subject to shearing due to lateral variations in flow velocity. To study these flows, we performed a series of PEG experiments in straight channels of uniform width, cross-section, and slope (Griffiths et al. 2003). During the experiments, we covered a wide parameter range by systematically varying the effusion rate, the channel width, the channel slope, and the cooling conditions. We found two distinctly different regimes of flow behavior (Fig. 3a and b). In the *tube* regime, a stationary solid crust covered the flow for most or all of its length, resulting in flow through an insulated tube. In the *mobile crust* regime, a solid crust was carried freely down the central part of the channel, separated from the channel walls by well-defined shear zones. A *transitional* regime showed some elements of both tube and mobile crust behavior, dependent on time and position along the channel.
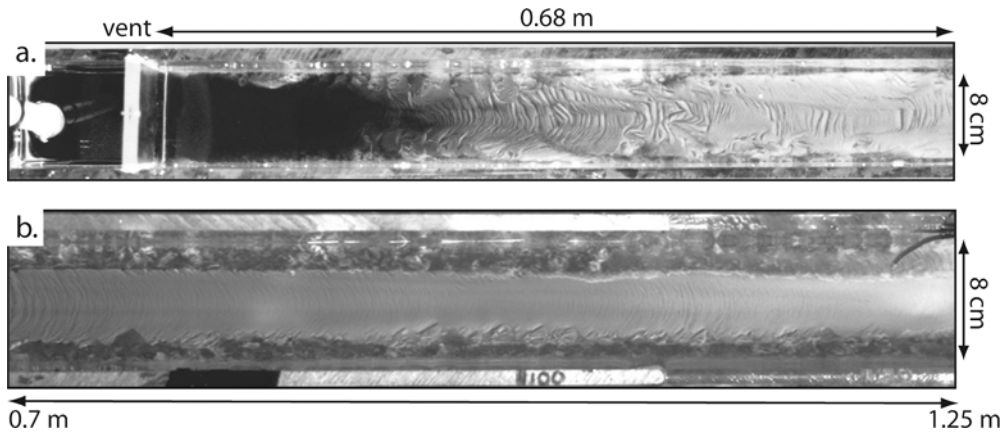
Fig. 3 Overhead views of two runs in the intermediate width channel (*W*=0.08 m). **a** 'Tube' flow under a rigid stationary crust (*Q*=2.5 cm³ s⁻¹, T_a=8.5°C, *r*=0.082, ψ=1.95, *Ra*=1.3×10⁵, ϑ=21.5, visible section along channel is *x*=−0.2 to 0.68 m); and **b** the 'mobile crust' regime with open shear layers in which only dis-persed solid occurs (*Q*=21 cm³ s⁻¹, T_a=4.6°C, *r*=0.165, ψ=2.67, *Ra*=9.5×10⁵, ϑ=56.5; *x*=0.70–1.25 m). The channel walls can be seen at the *top* and *bottom* of the images. The supply tube, lock, and sluice gate are included in (a). From Griffiths et al. (2003)

Flow regimes in our experiments can be simply described in terms of the variation with effusion rate, since decreasing the effusion rate has the same effect as increasing the channel width, decreasing the channel slope, or increasing the rate of cooling (see Eq. (1)). Tube flow occurred at small effusion rates (Fig. 3a). The lowest effusion rates produced a tube roof that formed at the vent and grew downstream. With increasing effusion rates, the roof formed at some distance down the channel, where rafts of solid jammed between channel walls, and then grew upstream toward the vent. Still higher effusion rates created a mobile crust (Fig. 3b) with a flow surface that remained free of continuous crust along each sidewall. With increasing effusion rates, the central crust decreased in average width and formed farther from the vent. Shear zones contained either roughly circular plates ('rosettes') or finely shredded solid. Vertical movement of fine solid fragments down the sidewall during down-channel flow showed that the flow was three-dimensional, probably as a consequence of thermally driven convection. Transitional flows formed at intermediate conditions. In the transitional regime, the widths of sidewall shear zones decreased with increasing distance from the vent, eventually disappearing so that the flow surface was covered with solid but was not stagnant, as in the true tube case. The expanding solid crust tended to restrict the flow in the channel, such that a characteristic of this regime was unsteady flow with periodic overriding of downstream crust by faster flows from upstream. The resulting internal stacking of liquid and solid greatly thickened downstream parts of the flow. Although this particular style of behavior is a consequence of the relatively high strength of the solid wax, flow thickening is anticipated under any conditions that reduce down-channel flow velocities relative to those upstream (e.g., Hon et al. 1994).

Parameterization

To parameterize conditions that define the two channel regimes, we used ψ to incorporate the effects of both

cooling and flow (Eq. (1)). For uniform channels of rectangular cross-section, H_0 and U_0 were defined as the depth and centerline velocity for viscous gravitational flow of an isoviscous (isothermal) liquid with a free surface (Tallarico and Dragoni 1999). We calculated a solidification time t_s using the methods of Griffiths and Fink (1997). Our experiments were conducted well within the laminar flow regime at low to moderate Reynolds numbers ($Re = U_0 H_0 / \nu_0 = 0.2$–30, where ν_0 is the kinematic viscosity of the fluid). On the basis of our observations of thermal convection along the length of the flow, we used the Rayleigh number (*Ra*) as a second dimensionless parameter:

$$Ra = \frac{g\alpha(T_e - T_s)H_0^3}{\kappa \nu_0}. \qquad (2)$$

Here *g* is the gravitational acceleration, and α, κ, T_e, and T_s are the fluid's thermal expansion coefficient, thermal diffusivity, initial temperature (that of the flow interior), and solidification temperature (that of the cooled liquid surface), respectively. The heat flux resulting from thermal convection can be approximated as $(Ra/R_0)^{1/3}$, where R_0 is a constant. If heat is lost only through the upper surface, Rayleigh numbers relevant to our PEG flows ($10^5 < Ra < 10^8$) suggest $R_0 \approx 100$ (for details of the parameterization see Griffiths et al. 2003).

A plot of all experiments as ψ versus *Ra* (Fig. 4a) shows complete separation of tube and mobile crust regimes such that for each value of *Ra*, tube behavior is found at small values of ψ (low effusion rates) and mobile crust behavior when ψ is large (rapid effusion rates). The transition between regimes occurs at smaller values of ψ for larger *Ra*, demonstrating that strong convection (large *Ra*) inhibits construction of a rigid roof across the channel and thus limits tube development. Experiments in which behavior was classified as transitional cluster near the boundary between
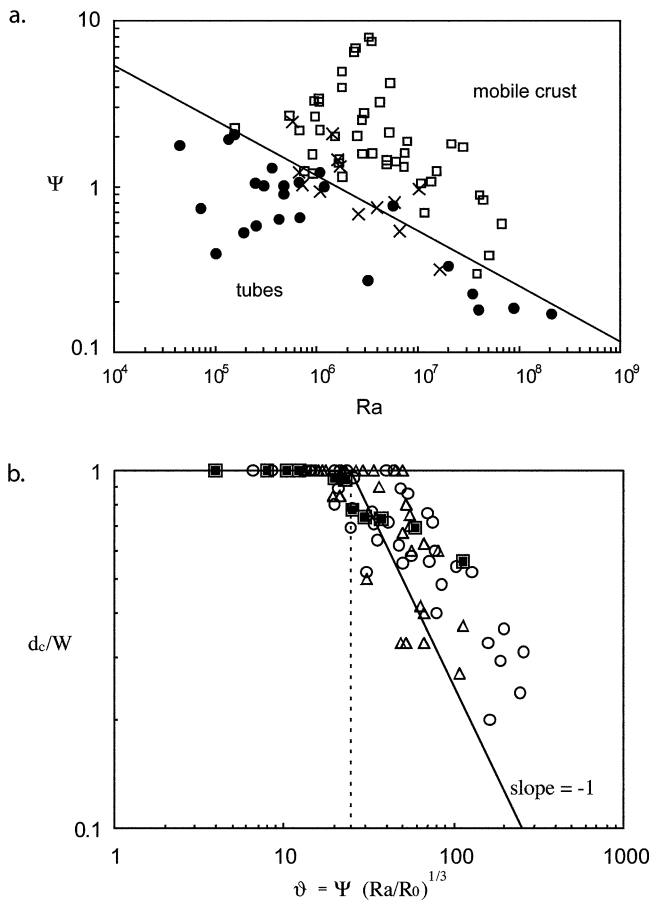
Fig. 4 **a** The experiments in $\psi - Ra$ space, along with their classifications as 'tube' flow ($\bullet$), 'mobile crust' flows ($\square$), and 'transitional' flows ($\times$). The empirical boundary between the 'tube' and 'mobile crust' regimes is given approximately by $\psi=(25\pm3)(Ra/R_0)^{-1/3}$ with $R_0=100$ (*solid line*), or, equivalently, $\vartheta=25\pm3$. **b** Width d_c of central mobile crust normalized by channel width W and plotted as a function of ϑ for three channel widths: ($\triangle$) $W=40$ mm; ($\circ$) $W=80$ mm; ($\blacksquare$) $W=150$ mm. From Griffiths et al. (2003)

tube and mobile crust regimes, constraining the transition to

$$\psi = (25 \pm 3)(Ra/R_0)^{-1/3}. \tag{3}$$

The results of Fig. 4a can be simply represented by a combined parameter

$$\vartheta = \psi(Ra/R_0)^{1/3}, \tag{4}$$

with the style of solidification given solely by the conditions:

$$\begin{array}{l} \vartheta < 25 \rightarrow \text{tube} \\ \vartheta > 25 \rightarrow \text{mobile crust.} \end{array} \tag{5}$$

In practice, Eq. (5) allows us to predict the flow regime for solidifying channelized flows from ψ (Eq. (1)) and the temperature difference driving thermal convection (assuming that the other intensive parameters of the flow are well

constrained). We also note that $\vartheta = U_0 t_s/\delta$, where δ is the thermal boundary layer thickness characteristic of convection at high Rayleigh numbers (Griffiths et al. 2003).

We can use the results of these experiments to predict crustal coverage (f_{crust}) of channelized flows in the mobile crust regime, where the width d_c of the central crust and the complementary width d_s ($=0.5-0.5d_c$) of the sidewall shear zones are well-defined properties of the flow. Figure 4b shows that the ratio of crust width-to-channel width d_c/W ($=f_{crust}$) increases with decreasing ϑ, reaching 1 at $\vartheta = \vartheta^* = 25 \pm 3$. Surprisingly, there is no apparent dependence of these normalized flow widths on the aspect ratio of the flow, which might be expected to influence the cross-channel profile of stream-wise shearing that, along with the convective heat flux from the interior, maintains the crust-free shear zones. Instead, although the data are scattered, the fraction of crustal coverage d_c/W appears to scale simply as ϑ^*/ϑ (Griffiths et al. 2003).

Basaltic lava channels

Two critical points emerging from the experiments of Griffiths et al. (2003) are that (1) thermal convection is important for maintaining crust-free sidewall shear zones, and (2) basic flow (lava velocity and depth) and thermal (lava temperature, thermal expansion, and diffusivity) parameters provide sufficient information to predict the extent of crust development on steady flows through uniform channels. These experimental results can be qualitatively compared with the observed behavior of basaltic lava channels from Mauna Loa (Lipman and Banks 1987; Crisp et al. 1994) and Kīlauea (Wolfe 1988; Kauahikaua et al. 1998; Cashman et al. 1999) volcanoes in Hawaii and from Etna Volcano, Sicily (Calvari et al. 1994; Calvari and Pinkerton 1998, 1999; Calvari et al. 2002; Harris and Neri 2002; Behncke and Neri 2003). The general observations that lava tubes are most common when effusion rates are low, and that central crusts are common features of open-channel flows, suggest qualitative agreement with the experimental results. Additional agreement comes from convective motions observed within lava channels (Booth and Self 1973), previously attributed to the combined effect of drag in sidewall shear zones and possible thermal convection.

A quantitative comparison of our experimental results with field observations may be made using documentation of open-channel flows from Mauna Loa, Hawaii in 1984 (Lipman and Banks 1987) and Mt. Etna, Sicily in 1991–1993 (Calvari et al. 1994). Griffiths et al. (2003) demonstrate that both Re and Ra values for basaltic lava flows are well covered by the experimental conditions investigated. In both settings, the channels are typically much longer than they are wide and wider than they are deep, with aspect ratios ($r=H/W$) between 0.5 and 0.05, also similar to our experimental flows. We can make a further comparison between our experiments and these lava flows by evaluating ψ and ϑ (Eqs. (1) and (4)). Using expressions given in Griffiths and Fink (1992), we calculate that $t_s\sim10$ s for proximal Mauna Loa lavas

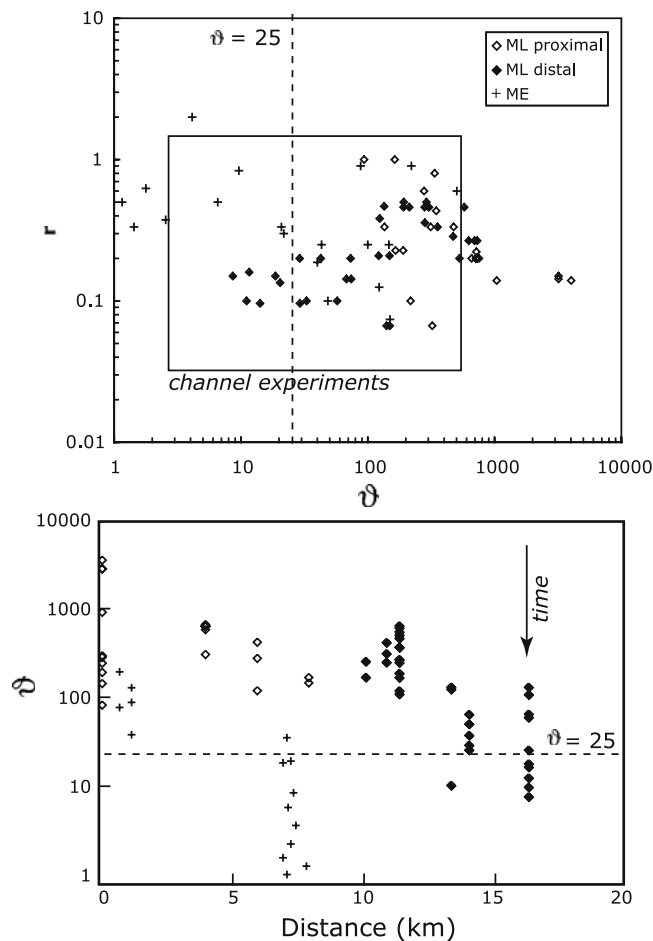**Fig. 5** (**a**) Channel aspect ratio r vs. ϑ for Mauna Loa 1984 and Etna 1992 channels. Data on channel dimensions and flow rates from Calvari et al. (1994) and Lipman and Banks (1987); ϑ calculated using Eqs. (1)–(4). (**b**) Down-flow variation in ϑ for the same flows. Symbols the same as in (a). Variation in ϑ at the same location shows variation through time (see *arrow* for general trend); in general, ϑ decreased as each eruption progressed

with high vesicularity and $1100°C \leq T_e \leq 1150°C$, and $t_s \sim 20$ s for Etnean and distal Mauna Loa lavas with lower vesicularities and temperatures. When combined with reported flow velocities and channel depths, these values of t_s yield $0.6 \leq \psi \leq 60$ and $10 \leq \vartheta \leq 3000$ for Mauna Loa, and $0.3 \leq \psi \leq 30$ and $1 \leq \vartheta \leq 220$ for Mount Etna.

A plot of r and ϑ shows that the parameter range of basaltic lava flows overlaps that of our experiments (Fig. 5a). Moreover, ϑ exceeds our experimentally determined critical value $\vartheta^* = 25$ for proximal and medial reaches of both Mauna Loa and Mount Etna flows, consistent with observed lava transport through open channels (our mobile crust regime). Additionally, Fig. 5b shows that ϑ decreases with both distance from the vent and eruption time as a consequence of diminishing flow velocities, eventually dropping below the critical value of 25 in distal reaches of both flows. Persistent low ϑ values in the distal part of the Etna flow during 1992 are consistent with observed lava tube formation in this part of the channel (Calvari and Pinkerton 1998). The applicability of our pa-

rameterization to basaltic flows is further supported by a recent analysis of flow conditions that produced submarine lava tubes and channels, which shows a good correspondence between experimentally identified flow regimes and those inferred from flow morphologies when plotted in either $\psi - Ra$ or $r - \vartheta$ space (Soule et al. 2005).

In summary, the general patterns of basaltic lava flow behavior are sufficiently similar to our experiments that ϑ should provide a useful parameterization of crustal coverage during channelized flow. However, two assumptions affect the direct application of our experimental results to basaltic lava channels. The first is that the erupted fluid that forms the flow core is Newtonian. This assumption is appropriate for proximal Hawaiian lava channels and submarine lava flows but may not apply directly to distal Hawaiian channels or Etna lavas, which contain sufficient crystals to produce non-Newtonian rheologies (Pinkerton and Sparks 1978; Fink and Zimbelman 1986, 1990; Moore 1987; Crisp et al. 1994; Cashman et al. 1999). Second, we have assumed that channels are straight, smooth, and uniform, clearly an over-simplification for real flows (e.g., Fig. 1). Here we address the latter problem by presenting the results of experiments with channel irregularities, including changes in channel width, sinuosity, and surface roughness. We then place these results in the context of existing models for channelized lava flows, paying particular attention to the effects of flow geometry on crustal coverage (cooling regime). To our knowledge, the effects of channel irregularities have not been explicitly addressed in models of either flow cooling or lava tube formation (e.g., Greeley 1987; Peterson et al. 1994; Crisp and Baloga 1994; Dragoni and Tallarico 1994; Kauahikaua et al. 1998; Harris and Rowland 2001; Crisci et al. 2004).

Experiments with irregular channels

Our experiments involved sustained releases of polyethylene glycol (grade 600) at a constant effusion rate and temperature in sloping, acrylic channels (cf. Griffiths et al. 2003; Fig. 6a). We used two different channels: our 'narrow' channel was 8 cm wide, our 'wide' channel was 15 cm in width. Cooling was achieved by releasing PEG beneath cold saline solutions. We investigated flow through four different types of channel irregularities: (a) Expanding channels (Fig. 6b); (b) contracting channels (Fig. 6c); (c) a meandering channel (Fig. 6d); and (d) a channel with bottom irregularities (Fig. 6e). During each experiment we monitored the water temperature T_a, PEG temperature T_e, and flow depth H. After each experiment we described and measured the crustal coverage from still photo and video footage. Throughout these experiments we attempted to cover the range of Re (0.6–20), Ra (10^5–10^7), r (0.1–1.2), and ϑ (10–115) used in the straight channel experiments of Griffiths et al. (2003).

An abrupt channel expansion was created by insertion of transparent acrylic sheets in the upper part of the narrow channel such that at the end of the insert, the flow

Fig. 6 **a** Sketch of the experimental apparatus. (Griffiths et al. 2003). From an overhead reservoir, polyethylene glycol (PEG) wax was gravity fed at a specified rate into the upper end of a sloping acrylic channel where it flowed under a sluice gate (the vent) and down the channel, traveling under cold salty water contained in an outer glass tank. The end of the channel was raised above the floor of the glass tank to provide a waste repository for the liquid and solid wax. Both overhead and side views of the experiments were recorded using video and still cameras. **b–e** Modifications to experimental setup. Plan view diagrams of (b) abrupt and gradual channel expansions; (c) abrupt and gradual channel constrictions; (d) meandering (zigzag) channel. (e) Shows a side view of channel obstructions. *Inset* shows parameter range of experiments
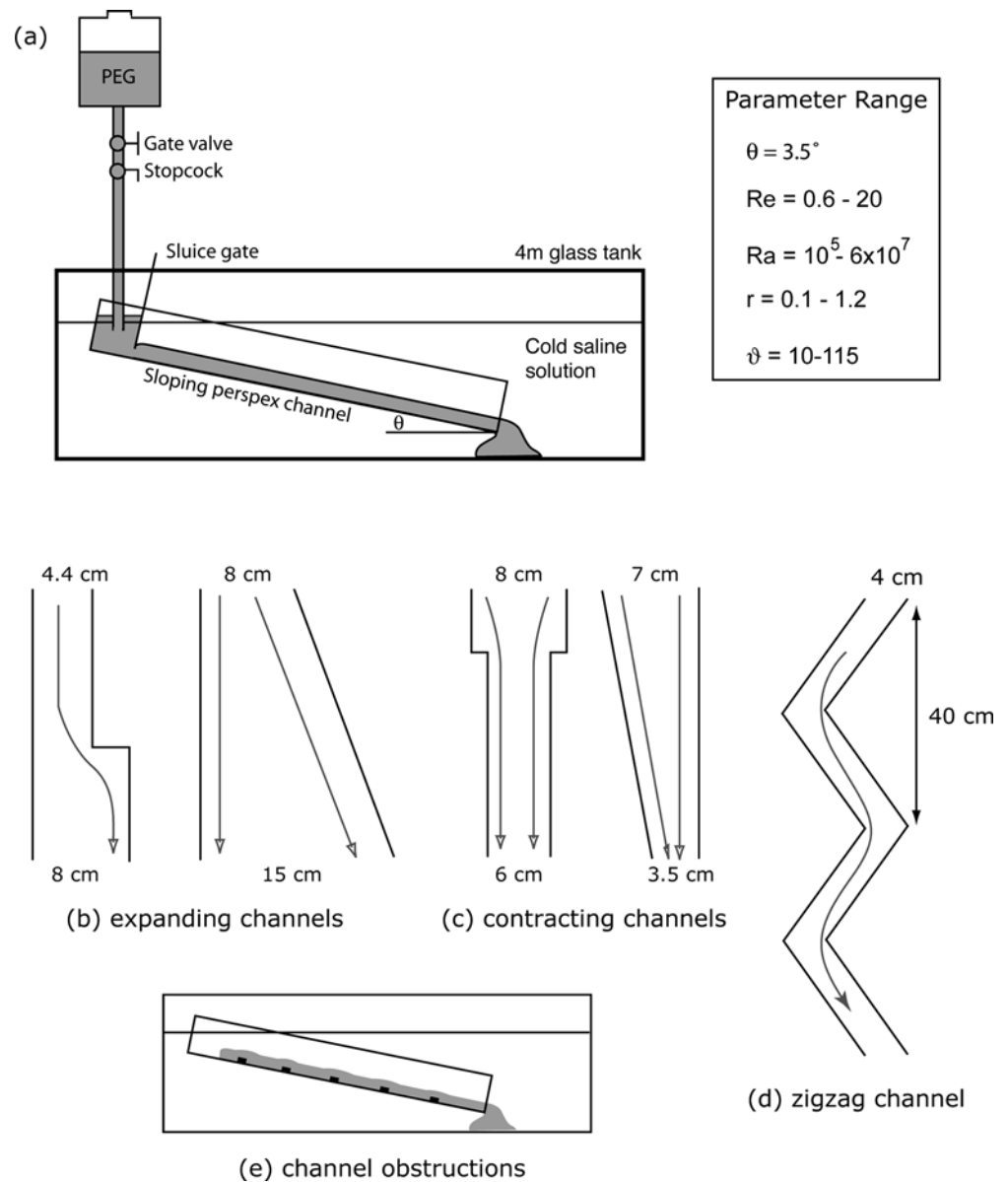
experienced an asymmetric step change from a width of 4.4 to 8 cm. An insert placed at an angle in the wide channel created a smooth asymmetric expansion from 8 to 14 cm over a distance of 1.7 m. Flow through a channel contraction was achieved by putting inserts in the narrow channel to generate a symmetric step decrease in channel width to 6 cm starting 0.65 m from the vent (Fig. 7b). Insertion of a barrier placed at an angle along the same channel created a gradual asymmetric contraction from 7 to 3.5 cm over 1.4 m. Meanders were created by inserting triangular pieces of acrylic into the narrow channel to yield a zigzag channel 1.2 m long, 4 cm wide, and with a meander wavelength of 0.4 m (Fig. 7c). Additionally, two experiments (one with cooling and one without) were performed in the zigzag channel to evaluate the role of thermal convection. Here continuous streams of dyed wax (emitted from 2 mm diameter tubes placed immediately inside the sluice gate) showed vertical and cross-stream motions of flow through the channel (e.g., Griffiths et al. 2003). Finally, we investigated the effect of bottom irregularities in the narrow channel, first by placing square ridges (1 cm high and 1 cm wide) perpendicular to the flow direction at 0.15 m intervals along the channel length, and second by placing 1.2 cm diameter metal tubing in a zigzag pattern (with a meander wavelength of 0.21 m) along the channel length.

Appearance of the flows

Expanding channels

Channel expansions resulted in a decrease in U_0 and hence ϑ. When the effusion rate was high (or the cooling was weak), large upstream ϑ values produced narrow solid crusts that traveled with unchanged width through the abrupt and asymmetric expansion and for some distance

Fig. 7 Photographs of expanding and contracting channel experiments. **a** Addition of thin crust to thicker central crust to accommodate channel expansion; **b** transitional behavior in a gradually expanding channel showing down-flow increase in crust coverage aided by rotation of solid rafts; **c** wide central crust jamming and backing up to form tube at channel constriction (insets that form constriction are outlined); **d** thin central crust traveling unaltered through gradually narrowing channel. In all photos down-channel direction is to the right
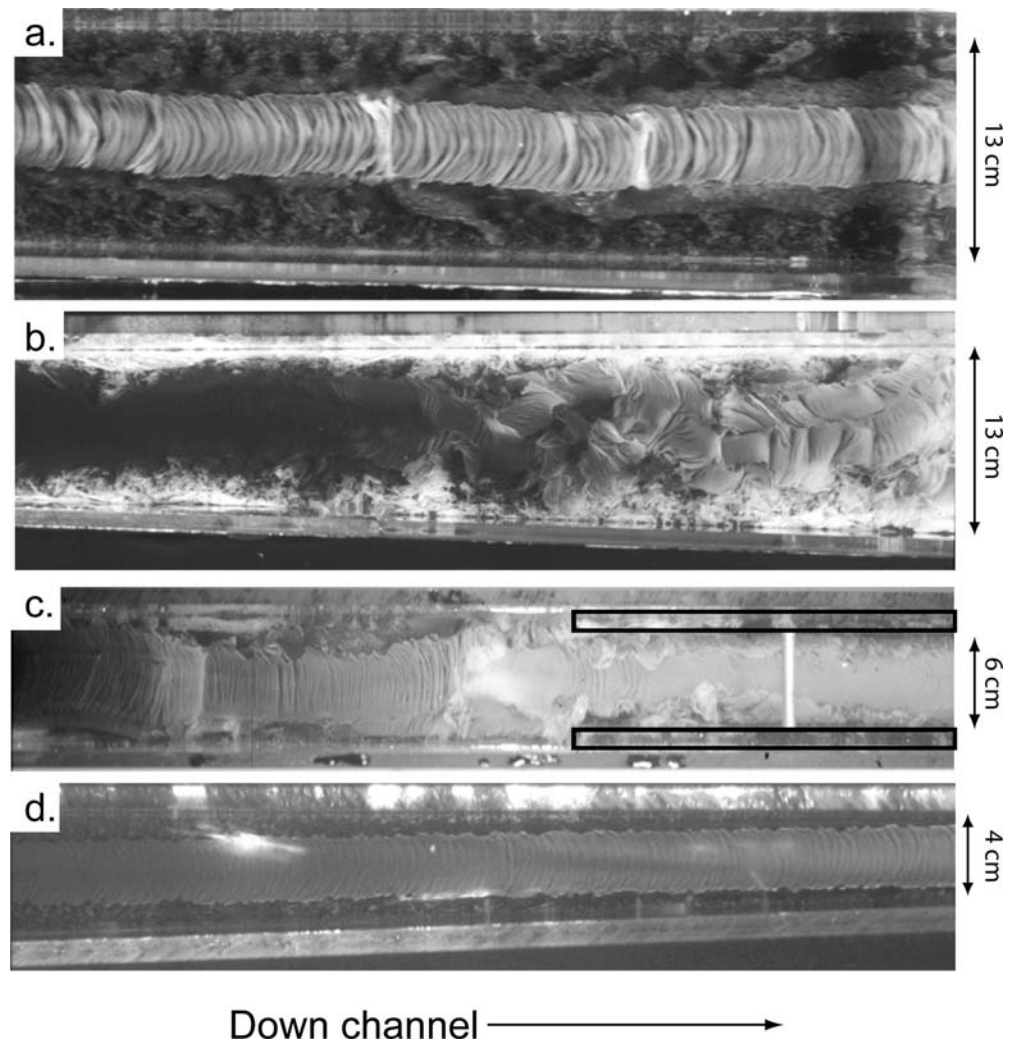
Down channel ⟶

down the channel. Additionally, strong flow divergence at the expansion (1) bent the crust towards the new center of the channel, (2) tore the margins of the crust, and (3) swept solid fragments within the shear zone to the new sidewall position. With lower effusion rates (or stronger cooling), a stagnant zone formed in the sharp corner of the channel at the divergence point. Surface solidification in this area generated a smooth transition from the narrow to the wide channel. Finally, when the initial effusion rate was sufficiently slow to form a tube in the narrow part of the channel, wax emerging from the narrow tube solidified rapidly to extend the tube across the wider part of the channel.

In the gradually expanding channel, surface crustal coverage changed continuously with channel width. At large ϑ (high initial effusion rates and/or weak cooling), the width of the central crust expanded with distance by accretion of solid material along the edge of the original central crust (Fig. 7a). When the effusion rate was reduced (or cooling strengthened; lower ϑ), the flow behavior was transitional, with the mobile central crust formed near the vent transforming with distance to a semi-rigid roof across the full width of the channel (Fig. 7b). Flow behavior under these conditions was analogous to the transitional regime

of straight channels, with faster moving solid rafts from the upper channel backing up against and thickening over the slower downstream flow. In contrast to the behavior of straight channels, however, channel expansion permitted the crustal rafts to rotate, eventually blocking the channel. In this way, a tube formed at the downstream of the channel and propagated upstream. Very low effusion rates caused a tube to form at the vent and to grow down the channel.

Contracting channels

An abrupt channel constriction caused local acceleration of the flow, producing an increase in ϑ. The effect of this acceleration on the flow depended on the width of the crust upstream of the constriction relative to the channel width at the constriction, as well as on the strength of the solidified crust. When the central crust was narrow (large ϑ) it passed easily through the constriction. However, flow acceleration created a region of local extension that broke both the central crust and rosettes from the sidewall shear zones into smaller pieces as they were swept into the narrower

Fig. 8 Photographs of meandering channel experiments. **a** For $\vartheta > 50$, a thin mobile crust travels easily through the zigzag channel, with minor crustal breakage and rotation ($\vartheta = 55$); **b** for $\vartheta < 50$, the channel flow exhibits transitional behavior and upstream-propagating tube formation ($\vartheta = 48$); **c** dye tracer experiment with no cooling; **d** dye tracer with cooling ($\vartheta = 58$). Dye tracer experiment shown in (c) shows flow exiting from zigzag channel into wider channel and rapid migration of dye to the channel walls. In comparison, when cooling accompanies flow (d) the dye tracers migrate vertically down the channel walls, then laterally into the middle of the channel
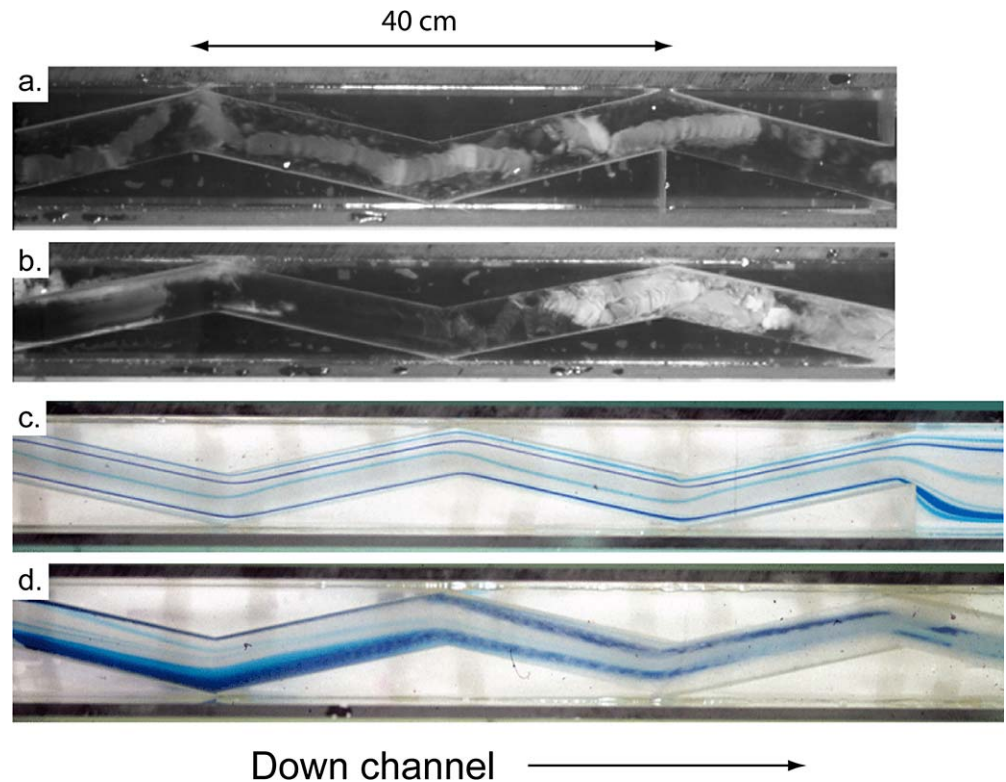
channel. With decreasing effusion rates (smaller ϑ), the width of the central crust above the constriction reached, and then surpassed, the width of the narrow part of the channel. When the crust width was close to or greater than that of the narrow channel, the crust caught at the constriction and rapidly backed up to form an upstream tube (Fig. 7c). When the crust width was slightly less than that of the constriction, crustal fragments created by local extension also rotated and blocked the channel entrance. In response to this blockage, the upstream flow thickened, overrode, and subsumed the fixed crust to form the stacked alternating sequences of solid and liquid layers characteristic of transitional flow regimes in straight channels (Griffiths et al. 2003).

In the gradually contracting channel, crust behavior again depended on effusion rate and crust strength. The highest effusion rates (largest ϑ) produced a well-developed central crust with finely disrupted wax in the shear zones. However, although we anticipated that the increase in ϑ caused by the decreased channel width should induce a reduction in crust width, instead we found that the crust width remained approximately constant. We believe that this lack of response is a consequence of the large strength of the pre-existing solidified PEG (e.g., Soule and Cashman 2004), which prohibited the tearing of crust margins required to diminish the crust width (Fig. 7d). The flow also became deeper and faster as the channel narrowed, causing some crustal extension and breakage. At lower effusion rates (smaller ϑ), the wide crust formed in the upper channel could not pass through the narrowing channel, causing it to jam and stacking behavior to begin. At the lowest effusion rates (lowest ϑ), tubes formed at the vent and extended down the channel.

Zigzag channels

Experiments in zigzag channels designed to simulate meanders showed similar features to flows in contracting channels, largely a result of differential acceleration of the flow around corners. When effusion rates were high (large ϑ), a thin mobile crust passed freely through the meanders, although acceleration around channel bends caused extensional breakage and accompanying rotation of broken fragments (Fig. 8a). When ϑ was small, a tube formed along the length of the channel. Intermediate effusion rates yielded transitional behavior, with broken crustal fragments rotating and blocking the channel, eventually creating upstream-propagating tubes (Fig. 8b).

Dyed wax released into the meandering channel allowed us to examine the role of thermal convection in this channel configuration. When there was no cooling, dyed wax released continuously near the surface remained parallel and at a fixed depth along the length of the channel (Fig. 8c). In contrast, cooling of the flow surface produced convective motions illustrated by the motion of the dyed wax outward and vertically down the sidewalls before converging toward the centerline down channel near the base of the flow (Fig. 8d). This convective behavior is similar to that observed in cooling straight channels (cf. Fig. 14 of Griffiths et al. 2003).

Bottom irregularities

Flow over a set of barriers placed across the bottom of the channel was characterized by alternating flow acceleration

Fig. 9 Photographs of experiments with bottom irregularities formed by square ridges (1 cm high and 1 cm wide) places across the flow at 0.15 m intervals. **a**, **b** At $\vartheta=70$, a narrow central surface crust forms near the source, which is broken by the accelerating flow over the ridges. The small pieces of broken crust then collide with each other and are scattered across the channel; **c**, **d** At $\vartheta=38$, a wide central surface crust forms near the source, which is also broken by the flow over the ridges. The large pieces of broken crust then collide with each other and are scattered across the channel
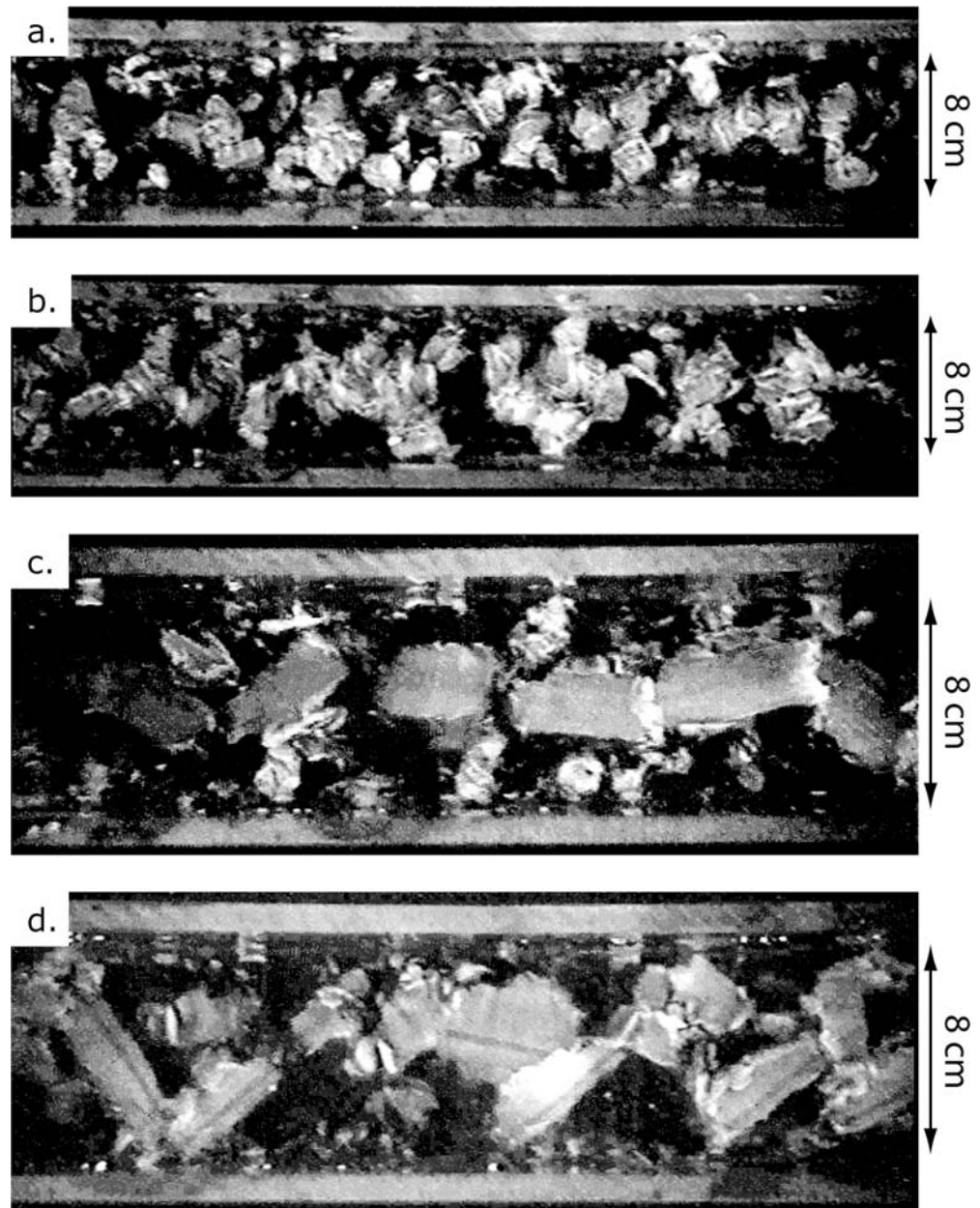
over each barrier and flow deceleration between barriers. When effusion rates were high and the central crust thin (large ϑ), this alternation in surface velocity broke the narrow surface crust at regular intervals and scattered small pieces of solid wax across the channel. The disrupted fragments rotated freely and moved easily down the channel (Fig. 9a and b). As effusion rates (and ϑ) decreased, the solid rafts increased in size (both width and length; Fig. 9c and d), interfering with each other during rotation and eventually clogging the end of the channel with solid debris. At this point, the entire surface moved as a rigid plug and the flow exhibited transitional characteristics. Very low effusion rates (small ϑ) gave tubes. In the mobile crust regime, the flow was uniform across the channel when barriers were placed perpendicular to the direction of flow but asymmetric when barriers were arranged in a zigzag pattern down

the length of the channel. For both types of bottom irregularities, the transition between the mobile crust and tube regimes occurred at $\vartheta^*=25\pm3$, as previously found for straight, uniform channels (Griffiths et al. 2003).

Analysis of experimental results

As demonstrated above, the basic flow regimes identified in the straight channel experiments of Griffiths et al. (2003) also describe flows through non-uniform channels (cf. Eqs. (3)–(5)). However, variations in the planform geometry changed the value of ϑ along the channel, thus allowing regime transitions despite a steady effusion rate and uniform slope. For example, at conditions of moderate ϑ, flow deceleration accompanying channel expansion
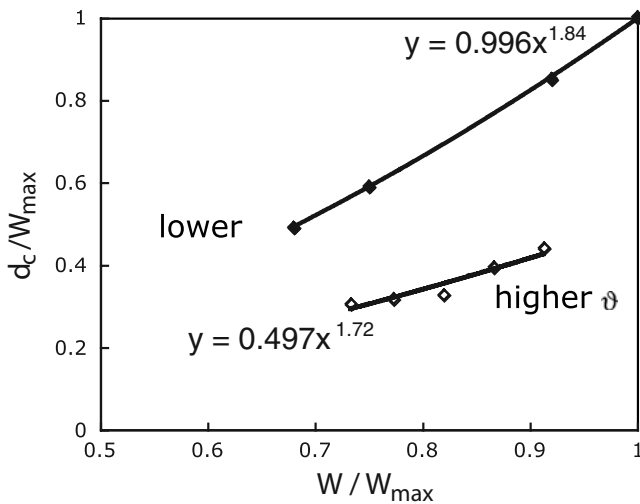
Fig. 10 Crust width (d_c) vs. channel width (W) for two gradual channel expansion experiments. Data normalized to maximum channel width W_{max}. Data shown in *open symbols* are for a higher flow rate than those in *closed symbols*. Power-law fit equations shown on figure; r^2 values are 0.905 for *open symbols*, 0.9998 for *closed symbols*

promoted transitional behavior as flow crusts stacked and thickened against slower downstream flows. When ϑ was close to ϑ^*, the decrease in ϑ resulting from the expansion was sufficient to permit downstream tube formation. Specifically, when ϑ decreased from 61 at the vent to 12 at the channel exit, tube formation began at about 0.9 m from the vent, where $\vartheta=23$. The transition between the mobile crust and tube regimes is therefore in reasonable agreement with the result ($\vartheta^*=25\pm3$) found for straight, uniform channels (Griffiths et al. 2003). The form of widening or narrowing (abrupt or gradual) was also important, as it modulated both the flow regime near transitional values of ϑ and the rate of crustal adjustment to new channel conditions. Finally, local flow acceleration produced by channel narrowing, bends, or bottom roughness served to disrupt the continuity of the surface crust. Resulting breakage and rotation of solid rafts often blocked the channel and created upstream-propagating tubes.

The descriptive analysis of experiments given above is most easily quantified for experiments in the gradually widening channel, where the surface crust widened by gradual accretion to the central crust established at the vent (Fig. 8a). To anticipate the crustal response, we use the parametric analysis of Griffiths et al. (2003) and assume that crust width d_c should vary with W as $d_c/W=\vartheta^*/\vartheta$ (e.g., Fig. 5b). We can also relate ϑ to the surface velocity U_0 as $\vartheta=U_0 t_s/\delta$. For shallow channels, the flow velocity and channel width are simply related to the flow depth H_0 by $U_0\sim H_0^2$ and $H_0\sim W^{-1/3}$. Substitution then yields $d_c/W\sim W^{2/3}$, or $d_c\sim W^{5/3}$, indicating that the fraction of surface covered by solid crust should increase in channel expansions and decrease with channel contractions as $W^{5/3}$.

We measured crust width along the gradually expanding channel for two different flow conditions, both of which started in the mobile crust regime. These measurements show that crust width increases with channel width as $d_c\sim W^{1.7-1.8}$ (Fig. 10), in very good agreement with the $W^{5/3}$ dependence predicted above. Additionally, at the lower effusion rate (smaller ϑ; upper curve of Fig. 10), d_c/W reached 1 by the channel exit and formed a tube. This change from mobile crust to tube flow is consistent with a calculated decrease in ϑ from 98 at the vent to 18 at the channel exit as a consequence of both the increase in channel width accompanying expansion and a small decrease in ambient water temperature along the channel. This analysis demonstrates that prediction of d_c is meaningful only for flow conditions that lie within the mobile crust regime. Figure 10 also illustrates that changes in ϑ (effusion rate) within the mobile crust regime are manifested by translation of curves along the d_c/W_{max} axis.

Changes in crust width were not the only modifications to the surface solid that we observed in our experiments. Also important was breakage and rotation of solid crusts as a consequence of abrupt acceleration of the flow through constrictions, over bottom irregularities, or around meander bends. At large ϑ, the continual disruption of the surface solid by irregularities was able to prevent the development of a continuous central surface crust. At smaller ϑ, the breakage and rotation of solid crusts created local blockages that aided upstream tube formation. From these observations, we conclude that local changes in channel width, sinuosity, and topography should play an important role in the overall thermal evolution of lava channels.

Application to basaltic lava channels

To what extent can the experimental results be applied to the behavior of basaltic lava flows? There are no published data to completely test our predictions. For example, Lipman and Banks (1987) provide sufficient data on channel and flow parameters to estimate ϑ, as shown in Fig. 6, but supply only qualitative descriptions of crust coverage of the flow surface along the channel. In contrast, the coverage of surface crust can be analyzed from published photographs of Kīlauea lava channels, but individual photographs typically lack specific information on channel dimensions or flow velocities. Later we use the latter source of information, making both qualitative and quantitative assessments of photographic evidence of surface crust behavior to link to the experimental results described above.

Qualitative observations

The behavior of surface crust is most easily observed on small Kīlauea lava channels where thin surface crusts form rapidly on crystal-poor lava flows as they emerge from vents or lava tubes (Fig. 11a–c). These crusts respond readily to small changes in applied stress, preserving information on the local kinematics of flow surfaces. For example, Fig. 11a provides a spectacular example of (1) longitudinal compression of the central crust as a small surface flow from Kīlauea Volcano (a ubiquitous feature of

Fig. 11 Photographs of active flows. **a** Small pahoehoe flow from Kilauea showing changes in both *flow* width and crust width as the flow travels over a break in slope. Note the well-developed shear zones along flow margins. Photo by DA Swanson, USGS. **b** Small surface breakout from pahoehoe flow, Kilauea Volcano, Hawaii. Note tearing of thin surface crust to accommodate spreading of flow and cooling of newly exposed lava. **c** Lava falls, Kupaianaha lava pond, Kilauea volcano (USGS photograph). **d** Aerial view of blockage developing along constriction in channel of 1984 Mauna Loa flow, March 31; flow direction is from *top* to *bottom* (photo from Lipman and Banks 1987). **e** Small lava channel at Mt. Etna active on March 3, 1999 near Southeast Crater. Channel is approximately 2 m in width; note narrow central crust despite low flow rate (<1 m s^{-1}). Photo by Boris Behncke
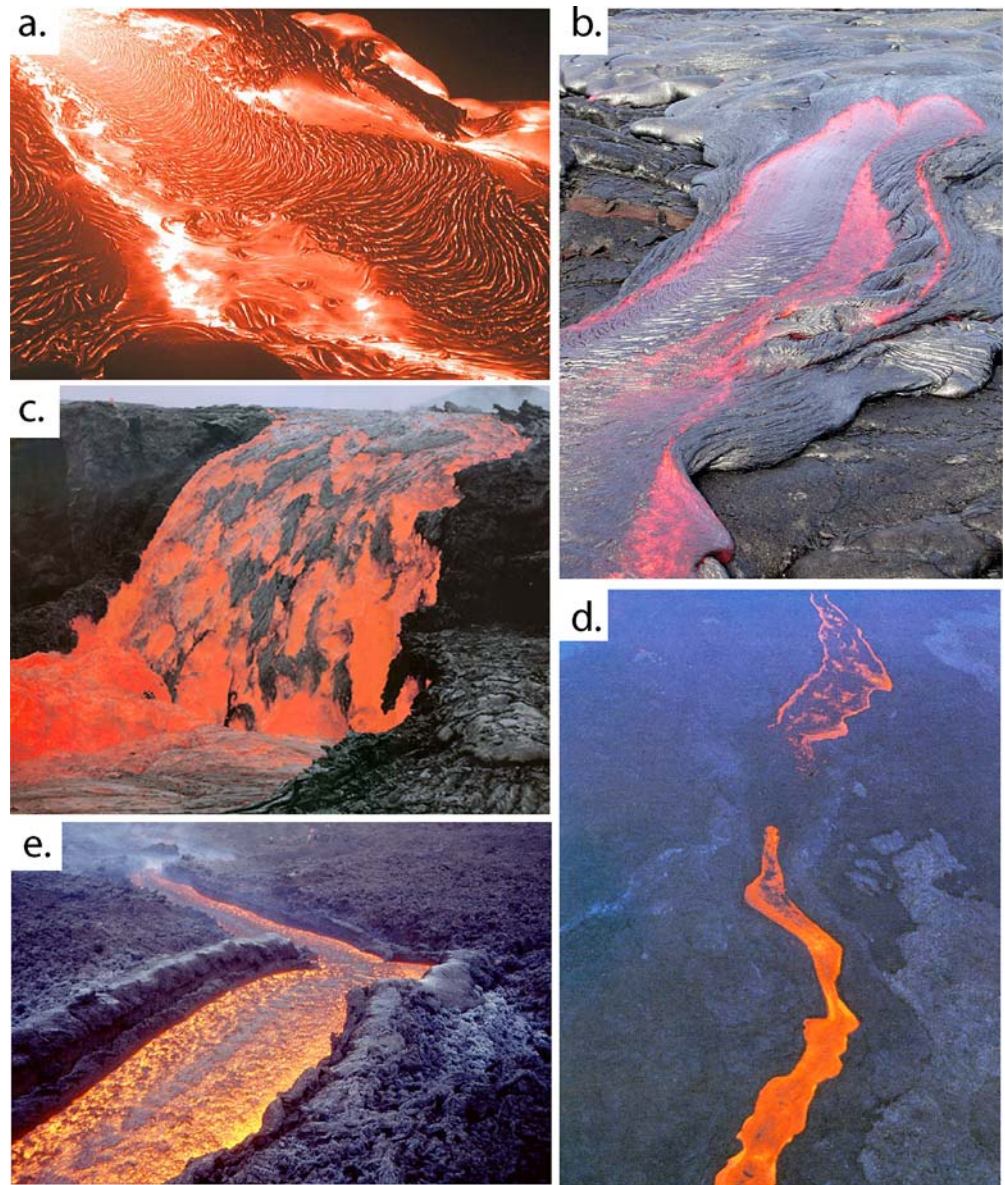
experimental mobile crusts (e.g., Fig. 3) and (2) prominent marginal rotating shear zones that change in width (first increasing, then decreasing) in response to changes in the flow geometry. Another response to flow expansion is shown in Fig. 11b, where a small breakout emerges and spreads laterally from a tube-fed Kīlauea flow. Here lateral expansion of the flow pulls the crust apart along a plane of pre-existing weakness parallel to the flow direction; the newly exposed flow surface in the middle of the flow then chills to form a continuous crust across the central flow surface, maintaining only narrow shear zones along the flow margins. In Fig. 11c, a small lava fall causes acceleration of the flow surface sufficient to completely disrupt thin crustal fragments. Submergence of the remnant crust within the plunge pool at the base of the lava falls creates a short down-flow region that is totally devoid of crust.

Less malleable are the ragged and broken crustal fragments that typify ʻaʻā flow surfaces. Figure 11d shows a channel segment of the 1984 Mauna Loa channelized flow (Lipman and Banks 1987) where a constriction has trapped ʻaʻā rubble, blocking the surface flow and causing a slow increase in both the width of the upstream flow and the width of the upstream surface crust. Emergence of lava from beneath the surface rubble exposes crust-free lava. An ʻaʻā flow from Mt. Etna (Fig. 11e) shows an increase in crustal coverage below the point at which lava emerges from a lava tube. Here the rough surface, and perhaps the narrowness of the channel crust, reflect Bingham rheology caused by the high crystallinity of Etna lava (e.g., Pinkerton and Norton 1995; Pompilio et al. 1998).

Quantitative analysis

Surface crust coverage can be analyzed from photographs that provide near-vertical views of lava channels. One such

Fig. 12 Channel produced by overflow of Mauna Ulu lava pond, February 28, 1972. Average channel width is approximately 10 m, flow direction is from *upper left* to *bottom right* (from Tilling et al. 1987)

photograph (Fig. 12; Tilling et al. 1987) shows a 150–200 m long section of an ∼10 m-wide lava channel that was produced on February 28, 1972, by an overflow from the Mauna Ulu lava lake, Kīlauea Volcano. The general appearance of the crust bears out our prediction that the fraction of surface coverage varies with changes in channel width. Moreover, crust width appears to change rapidly in response to changing geometry, with crust growth lagging behind channel expansion only when changes in channel width are moderately abrupt, as seen in the bottom right-hand corner of the photograph.

When analyzed as a whole, this channel has an average fraction of incandescent lava $f=0.20$. Here we count as 'incandescent' all colors from red to yellow, while 'crust' includes only the near-black portions of the channel. Individual transects perpendicular to the flow direction provide measurements of d_c and W along the length of the channel. Measurements were made at approximately even intervals that were sufficiently closely spaced to capture the channel response to observed variations in channel width. Consistent with the whole flow data, crustal coverage d_c/W measured over 16 representative sections averages 0.81 and varies from 0.69 to 0.92 from the narrowest to the widest parts of the channel. The generally high values of d_c/W suggest that the flow conditions were approaching values suitable for lava tube formation. If we use a mean channel width of 10 m, an average effusion rate of ∼2 m^3 s^{-1} reported by Tilling et al. (1987) for the 901 days of Mauna Ulu activity, and assume a slope of 3° and $t_s=10$ s, we calculate $\vartheta \sim 25$, indicating near-critical conditions for tubes. Although it is difficult to estimate the error on this value, a factor of two increase in the effusion rate would increase

our estimate of ϑ to about 40. A plot of d_c versus W shows that, as anticipated, d_c increases more rapidly than W. This relationship can be fitted by a power-law relationship with an exponent of 1.3 (Fig. 13a). This value is reasonably close to the 5/3 predicted by scaling analysis under the assumption of a volumetric flow rate independent of the distance along the channel.

A somewhat more complex channel produced during Episode 5 (July 1, 1983) of the ongoing Pu`u `O`o eruption of Kīlauea Volcano is shown in Fig. 14. Wolfe (1988) estimated the lava flow rate through this channel to be ∼100,000 m^3 h^{-1} (28 m^3 s^{-1}), with surface velocities of 1.25–1.5 m s^{-1} in the upper channel reaches. These flow parameters suggest a high initial value of ϑ (∼175), consistent with both open-channel flow and the narrow central crust evident near the vent. Midway down the channel a narrow section has completely roofed over, apparently the result of blockage by large rafted fragments at a channel constriction (e.g., Fig. 11d). Below this blockage the channel geometry changes dramatically, most noticeably in forming an impressive hairpin bend at a distance of about 1.5 km from the vent. Crust coverage varies extensively along this part of the channel, increasing through channel expansions and decreasing through channel contractions. Importantly, this variation includes abundant evidence of crustal breakage resulting from acceleration and extension of the flow. The result is an overall increase in the amount of incandescent lava exposed to radiative cooling. This effect is particularly evident in the hairpin bend, where the surface crust is completely disrupted ($f=1$). We note, however, that a region of highly disrupted crust just before the most distal channel expansion (labeled 'exp 2' in Fig. 14) cannot be explained
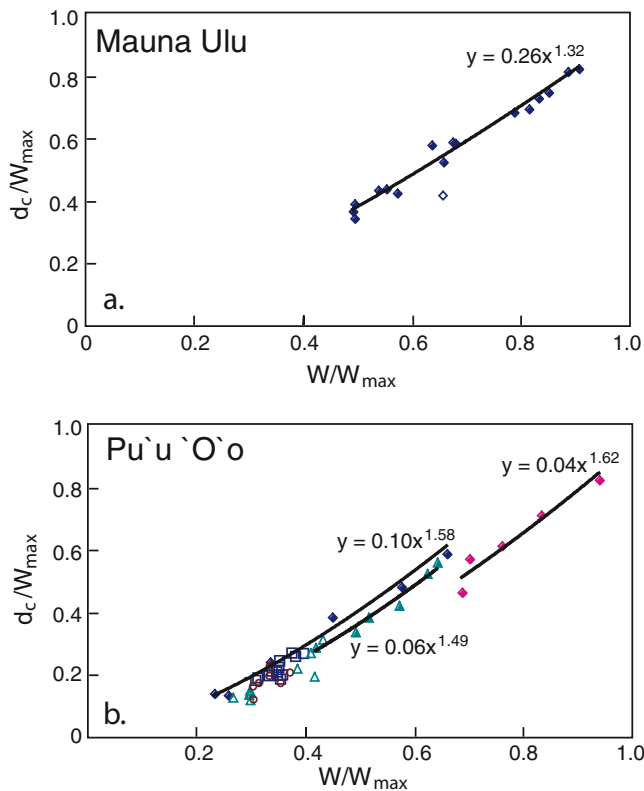
Fig. 13 Measured crust width (d_c) vs. W for **a** Mauna Ulu and **b** Pu'u'O'o channels. Widths are normalized to maximum channel width (W_{max}). Power-law fits to data are provided on plots; all fits have $r^2 \geq 0.98$. In (a), measurement represented by the *open diamond* was omitted from the curve fit. In (b), fits are shown for expansion 1 (*medium gray diamonds*), expansion 2 (*dark gray diamonds*), and the contraction (*medium gray triangles*); area encompassed by each channel segment is shown in Fig. 14

by changes in channel width or planform geometry. We suspect that exposure of incandescent lava at this location is a consequence of an abrupt change in slope (a lava fall).

Quantitative analysis of Fig. 14 is complicated by the photographic angle, which is not vertical. To reduce the problem of perspective and to examine the effects of different morphological changes, we divided the channel into six different segments for analysis. These segments include two widening channel segments (labeled 'exp 1' and 'exp 2'), one segment that narrows abruptly (labeled 'contraction'), one that narrows gradually (labeled 'narrowing'), one straight segment, and one that includes the spectacular hairpin bend. The average fraction of incandescent lava within each segment (f) varies from 0.31 to 0.80 (Fig. 13). Moderate crustal coverage is consistent with the high initial ϑ determined above. In contrast to the Mauna Ulu channel, however, measurements of crust width along a total of 46 cross-sections in the six segments yield d_c/W values that are consistently 10–20% higher than corresponding values of $1-f$ for the relevant channel segment (Fig. 15). This mismatch shows that crust width, alone, is not an accurate measure of the amount of incandescent lava exposed at the surface when there is also significant crustal extension and breakage along the channel. The effect of crustal disrup-

tion is most evident along narrowing and meandering parts of the channel, consistent with observations in our experiments. Only three channel segments (two expansions and one contraction) exhibit sufficient variation in W to obtain good power-law fits to trends of d_c versus W (Fig. 13b). Of these, exp 1 yields $d_c \sim W^{1.5}$ and both the contraction and exp 2 yield $d_c \sim W^{1.6}$. Together, these data are in remarkable agreement with our theoretical prediction of $d_c \sim W^{5/3}$.

Applications to models of lava flow behavior

Comparison of the behavior of basaltic lava channels with our analog experiments allows us to re-examine models of open-channel flow and lava tube formation. We show how our experiments (1) aid interpretation of observed flow features in both regimes, (2) supply a theoretical link between thermal and dynamical models of flow evolution, and (3) illustrate ways in which channel geometry may affect rates of flow cooling and styles of flow advance.

First and foremost, we have demonstrated the applicability of the simple ϑ parameterization of Griffiths et al. (2003) to define flow conditions that produce open-channel versus tube formation in basaltic lava flows. We have also shown ways in which this parameterization requires modification to accommodate the effects of local changes in channel geometry on the development of surface crust. Second, we have demonstrated that, along channels that are either uniform or slowly varying in geometry, the fraction of the flow covered by a solid crust (d_c) is a predictable function of flow width (W). These calculations of ϑ and d_c/W can easily be incorporated into existing flow models to add a more robust prediction of crustal coverage than exists currently. Third, both our experiments and our photographic analysis illustrate that crustal extension and breakage is common in non-uniform channels where local flow conditions accelerate the flow surface, such as channel constrictions, flow around bends, and flow over lava falls. Under these conditions the increased fraction of incandescent lava exposed at the flow surface will generate more rapid cooling than anticipated for similar flows in uniform channels. When coupled with models of crust growth and failure criteria, the insights into dynamic processes affecting crust distribution provided by our experiments could greatly improve predictions of flow cooling.

Our experiments also aid in the understanding of lava tube formation. Conditions leading to the development of lava tubes have been examined in both Hawaiian and Etna lava flows (e.g., Guest et al. 1980, 1984; Greeley 1987; Peterson et al. 1994; Hon et al. 1994; Calvari and Pinkerton 1998, 1999; Kauahikaua et al. 1998, 2003). According to these studies, processes by which lava tubes form include: (1) growth of lava crusts across streams within confined channels, (2) gradual accretion of lava levees, (3) coalescence of rafted solid plates, (4) progressive extension of pahoehoe lobes, and (5) inward focusing of lava in inflated sheet flows. Tube formation may initiate at the distal end of flows, near the vent, or within narrow sections of channels. While most common in pahoehoe flow fields that develop

Fig. 14 Pu'u'O'o channel July 1, 1983. Shown are analyzed segments with names used in text and average fraction of exposed lava core (*f*) determined by image analysis of each segment. Photo from Wolfe (1988)
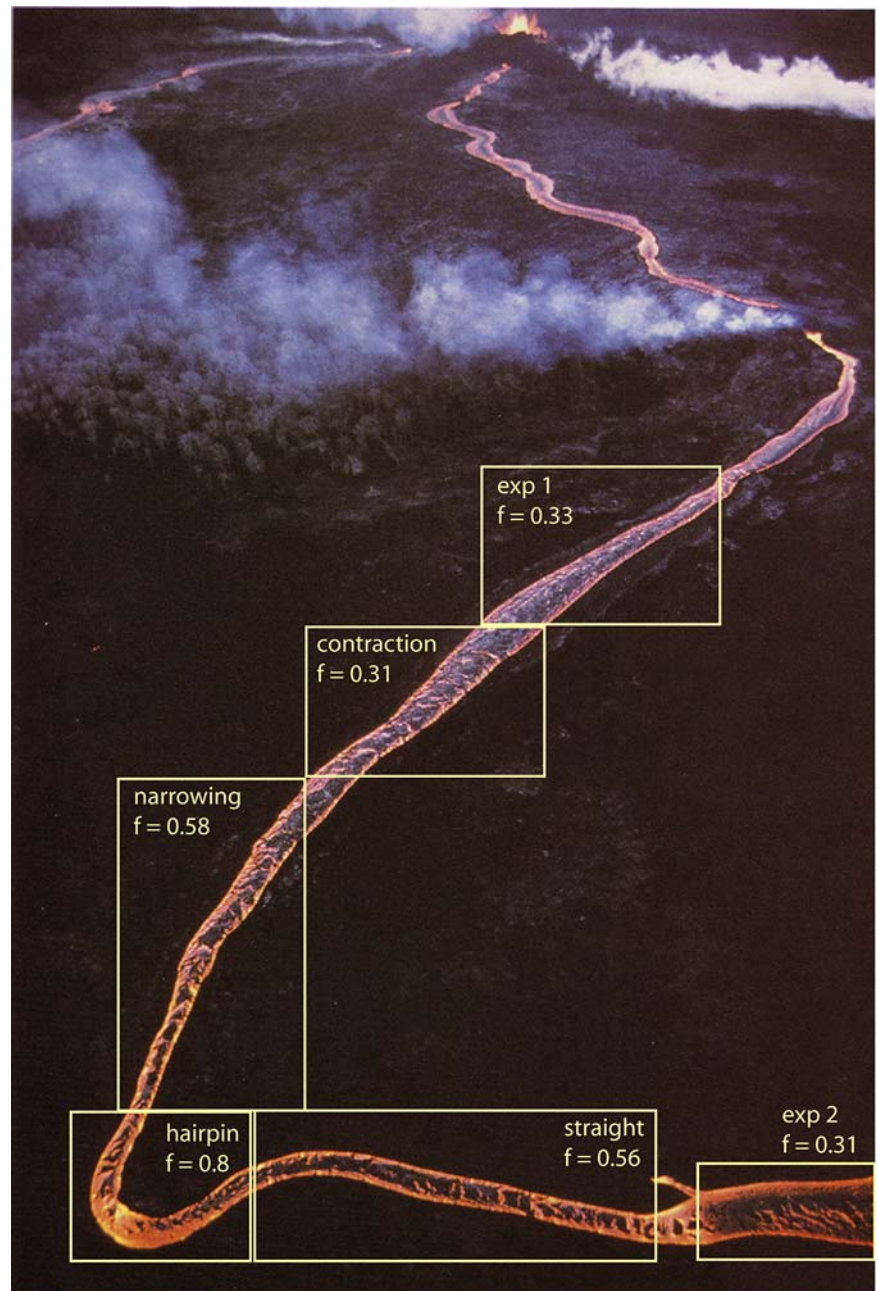
under steady and generally low volumetric effusion rates (e.g., Hon et al. 1994; Kauahikaua et al. 1998, 2003), tube formation has also been documented within 'a'a flow fields, again when flow is steady (e.g., Calvari and Pinkerton 1998, 1999; Kauahikaua et al. 2003).

Cooling flows in straight uniform channels gives rise to two different modes of tube formation dependent on ϑ (Griffiths et al. 2003). At low ϑ, solidification is rapid and tubes initiate near the vent area before propagating downflow. In contrast, at moderate (transitional) values of ϑ, the surface crust gradually expands in width during flow down the channel until it stalls against the channel margins. At this point stacking behavior commences, and, given sufficient time, tubes form at the far end of the channel and propagate up-flow. Similar tube initiation in distal channels of

lava flows of Mt. Etna in 1992 (e.g., Calvari et al. 1994; Calvari and Pinkerton 1998) occurred when maximum values of ϑ were close to our predicted transition values (Fig. 5).

Additional constraints on tube formation are provided by our experiments in non-uniform channels, where changes in channel geometry commonly promote tube formation when flow conditions are close to transitional values ($\vartheta \sim \vartheta^*$). Channel expansion can create lava tubes when widening of the channel is sufficient to cause ϑ to drop below ϑ^*. The same effect should be seen with slope reduction, although we did not attempt to simulate this transition. Channel constrictions may cause tubes to form in medial portions of the channel if the channel becomes too narrow to allow unfettered passage of solidified lava crusts. In this case, tubes initiated at the constriction propagate up-flow, as observed
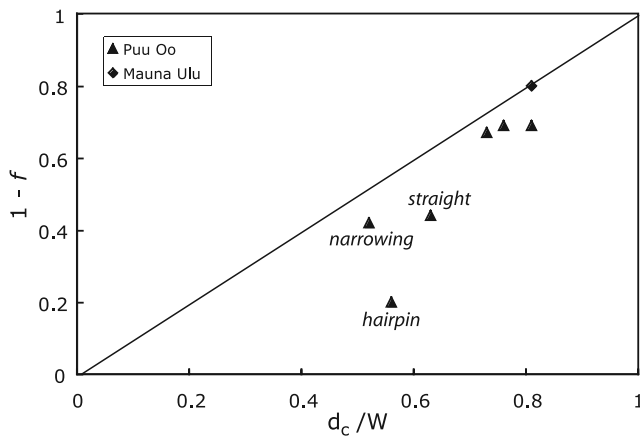
Fig. 15 Comparison of average measured ratios of crust width-to-channel width with the average total crustal coverage $(1-f)$ for individual channel segments shown in Figs. 12 and 14. Mismatch between the two values (shown as departure from the one:one line) is a measure of crustal disruption provided by crustal extension caused by flow acceleration. Labeled points indicate channel segments in Fig. 14 with comparatively large amounts of crustal extension because of acceleration around channel bends (*hairpin*), through narrowing parts of the channel (*narrowing*) and over breaks in slope (*straight*)

in Hawaiian lava channels (Fig. 14; Peterson et al. 1994). Constrictions and meanders may also promote tube formation when rafts of solidified crust rotate to block the channel. Such a process may aid the coalescence and welding of crustal blocks observed during tube formation at Mauna Ulu, Hawai'i and Mt. Etna, Sicily (Peterson et al. 1994; Calvari and Pinkerton 1998). Taken together, both our experiments and our photographic analysis of basaltic lava flows from Hawaii illustrate the importance of considering local changes in channel geometry in the development of accurate lava flow and cooling models.

Conclusions

Griffiths et al. (2003) demonstrate that there are critical conditions under which solidifying flows through straight, uniform channels develop either a continuous roof $(\vartheta < 25)$ or a mobile crust $(\vartheta > 25)$. They also show that vertical and cross-stream transport resulting from organized thermal convection is critical for the maintenance of crust-free shear zones over large down-channel distances. In this paper, we have tested these results by analysis of well-documented channelized basaltic lava flows from Mauna Loa, Hawai'i, and Mt. Etna, Sicily, and shown that the critical value of ϑ appears to be similar in field settings.

To address some of the complications arising from actual flow conditions, we performed an additional set of experiments in channels with non-uniform geometries. When the channel width increased, or was straight but contained bottom irregularities, $\vartheta^* = 25 \pm 3$ remained a good predictor of the transition between the mobile crust and tube regimes. Channel expansion promoted transitional behavior as flow crusts stacked and thickened against slower downstream flows. Constrictions and meander bends produced

upstream-propagating tubes when broken crustal rafts were sufficiently strong to block the channel. Analysis of channel expansion experiments confirms our prediction that in shallow channels, the central crust width (d_c) will change with channel width (W) as $d_c \sim W^{5/3}$ for a given volumetric flow rate. Moreover, the same relationship appears to hold for channelized lava flows from Hawai'i. Additionally, an important observation from our experiments is the role of crustal breakage and extension in increasing the amount of core fluid exposed at the flow surface. Breakage occurs with local acceleration of the flow surface through constrictions, around bends, or over bottom irregularities. These results could be easily tested and extended through direct measurements of channel velocities combined with FLIR imaging to determine crustal coverage (e.g., Pinkerton et al. 2002) and LiDAR imaging to characterize channel geometry (e.g., Mazzarini et al. 2005).

In basaltic lava channels, the effects of expansions and contractions appear reversible under most circumstances, in the sense that crust width approximates equilibrium values. Situations where this is not true include locations where changes in channel width are rapid or where the crust is broken extensively. Flows may also change from mobile crust to tube regime (or vice versa) at a constant effusion rate and slope simply from local changes in the width of the channel. Tubes may propagate upstream or downstream depending on specific values of ϑ. Downstream-propagating tubes are indicative of $\vartheta \ll \vartheta^*$, while upstream-propagating tubes form when the local channel geometry allows blockage of surface flow by crustal fragments. Thus, we conclude that channel geometry plays an important role in determining conditions of flow emplacement, particularly with regard to the stability or disruption of solid surface crusts. Finally, we note two important limitations of our experiments relative to real flows. First, the PEG wax used, when liquid, is a Newtonian fluid that may not be an adequate analog for the highly crystalline (Bingham) lavas typical of distal Hawaiian channels and most Etna flows. Second, all of our experiments were performed in rigid channels and thus provide no information on fundamental questions about channel formation and the processes governing channel geometry. These two areas provide directions for future research.

References

Behncke B, Neri M (2003) Cycles and trends in the recent eruptive behaviour of Mount Etna (Italy). Can J Earth Sci 40:1405–1411

Booth B, Self S (1973) Rheological features of the 1971 Mount Etna lavas. Philos Trans R Soc Lond A 274:99–106

Calvari S, Coltelli M, Neri M, Pompilio M, Scribano V (1994) The 1991–1993 Etna eruption: Chronology and geological observations. Acta Vulcanol 4:1–15

Calvari S, Pinkerton H (1998) Formation of lava tubes and extensive flow field during the 1991–1993 eruption of Mount Etna. J Geophys Res 103:27291–27301

Calvari S, Pinkerton H (1999) Lava tube morphology on Etna and evidence for lava flow emplacement mechanisms. J Volcanol Geotherm Res 90:263–280

Calvari S, Neri M, Pinkerton H (2002) Effusion rate estimates during the 1999 summit eruption on Mount Etna, and growth of two distinct lava flow fields. J Volcanol Geotherm Res 119:107–123

Cashman KV, Mangan MT, Newman S (1994) Surface degassing and modifications to vesicle size distributions in Kilauea basalt. J Volcanol Geotherm Res 61:45–68

Cashman KV, Thornber CR, Kauahikaua JP (1999) Cooling and crystallization of lava in open channels, and the transition of pahoehoe lava to 'a'a. Bull Volcanol 61:306–323

Crisci GM, Rongo R, DiGregorio S, Spataro W (2004) The simulation model SCIARA: The 1991 and 2001 lava flows at Mount Etna. J Volcanol Geotherm Res 132:253–267

Crisp J, Baloga S (1990) A model for lava flows with two thermal components. J Geophys Res 95:1255–1270

Crisp J, Baloga S (1994) Influence of crystallization and entrainment of cooler material on the emplacement of basaltic aa lava flows. J Geophys Res 95:1255–1270

Crisp J, Cashman KV, Bonini JA, Hougen SB, Pieri D (1994) Crystallization history of the 1984 Mauna Loa flow. J Geophys Res 99:7177–7198

Dragoni M, Tallarico A (1994) The effect of crystallization on the rheology and dynamics of lava flows. J Volcanol Geotherm Res 59:241–252

Dutton CE (1884) The Hawaiian volcanoes. US Geol Surv 4th Ann Rep, Government Printing Office, pp 75–219

Fink JH, Griffiths RW (1990) Radial spreading of viscous-gravity currents with solidifying crust. J Fluid Mech 221:485–510

Fink JH, Griffiths RW (1992) A laboratory analog study of the morphology of lava flows extruded from point and line sources. J Volcanol Geotherm Res 54:19–32

Fink JH, Zimbelman JR (1986) Rheology of the 1983 Royal Gardens basalt flows, Kilauea Volcano, Hawaii. Bull Volcanol 48:87–96

Fink JH, Zimbelman JR (1990) Longitudinal variations in rheological properties of lavas: Pu Oo Basalt Flows, Kilauea Volcano, Hawaii. In: Fink JH (ed) Lava flows and domes. Springer, Berlin Heidelberg New York, pp 157–173

Gregg TKP, Fink JH (2000) A laboratory investigation into the effects of slope on lava flow morphology. J Volcanol Geothermal Res 96:145–159

Greeley R (1987) The role of lava tubes in Hawaiian volcanoes. US Geol Surv Prof Pap 1350:1589–1602

Griffiths RW (2000) The dynamics of lava flows. Annu Rev Fluid Mech 32:477–518

Griffiths RW, Fink JH (1992) The morphology of lava flows under planetary environments: Predictions from analog experiments. J Geophys Res 97:19739–19748

Griffiths RW, Fink JH (1993) Effects of surface cooling on the spreading of lava flows and domes. J Fluid Mech 252:667–702

Griffiths RW, Fink JH (1997) Solidifying Bingham extrusions: A model for the growth of silicic lava domes. J Fluid Mech 347:13–36

Griffiths RW, Kerr RC, Cashman KV (2003) Patterns of solidification in channel flows with surface cooling. J Fluid Mech 496:33–62

Guest JE, Underwood JR, Greeley R (1980) The role of lava tubes in flows from Observatory Vent, 1971 eruption at Mount Etna, Sicily. Bull Volcanol 47:635–648

Guest JE, Wood C, Greeley R (1984) Lava tubes, terraces and megatumuli on the 1614–1624 pahoehoe lava flow field, Mount Etna. Geol Mag 117:601–606

Guest JE, Kilburn CRJ, Pinkerton H, Duncan AM (1987) The evolution of lava flow-fields: Observations of the 1981 and 1993 eruptions of Mount Etna, Sicily. Bull Volcanol 49:527–540

Harris AJL, Rowland SK (2001) FLOWGO: A kinematic thermorheological model for lava flowing in a channel. Bull Volcanol 63:20–44

Harris AJL, Neri M (2002) Volumetric observations during paroxysmal eruptions at Mount Etna: Pressurized drainage of a shallow chamber or pulsed magma supply? J Volcanol Geotherm Res 116:79–95

Helz RT, Banks NG, Heliker C, Neal CA, Wolfe EW (1995) Comparative geothermometry of recent Hawaiian eruptions. J Geophys Res 100:17637–17657

Helz RT, Heliker C, Hon K, Mangan M (2003) Thermal efficiency of lava tubes in the Pu'u `O`o-Kupaianaha eruption. US Geol Surv Prof Pap 1676:105–120

Holcomb RT (1987) Eruptive history and long-term behavior of Kilauea Volcano. US Geol Surv Prof Pap 1350:261–350

Hon K, Kauahikaua JP, Denlinger R, Mackay K (1994) Emplacement and inflation of pahoehoe sheets: Observations and measurements of active lava flows on Kilauea Volcano, Hawaii. Geol Soc Am Bull 106:351–370

Hon KA, Gansecki C, Kauahikaua J (2003) The transition from 'a'ā to pahoehoe crust on flows emplaced during the Pu'u 'O'o-Kupaianaha eruption. US Geol Surv Prof Pap 1676:89–104

Hulme G (1974) The interpretation of lava flow morphology. Geophys J R Astr Soc 39:361–383

Kauahikaua JP, Cashman KV, Mattox TN, Hon K, Heliker CC, Mangan MT, Thornber CR (1998) Observations on basaltic lava streams in tubes from Kilauea Volcano, Hawaii. J Geophys Res 103:27303–27324

Kauahikaua JP, Sherrod D, Cashman K, Heliker C, Hon K, Mattox T, Johnson J (2003) Hawaiian lava-flow dynamics during the Pu'u 'O'o -Kupaianaha eruption: A tale of two decades. US Geol Surv Prof Pap 1676:63–87

Kerr RC (2001) Thermal erosion by laminar lava flows. J Geophys Res 106:26453–26465

Keszthelyi L (1995) A preliminary thermal budget for lava tubes on the Earth and planets. J Geophys Res 100:20411–20420

Keszthelyi L, Denlinger R (1996) The initial cooling of pahoehoe flow lobes. J Volcanol Geotherm Res 58:5–18

Kilburn CRJ (1996) Patterns and predictability in the emplacement of subaerial lava flows and flow fields. In: Scarpa C, Tilling R (eds) Monitoring and mitigation of volcano hazards. Springer-Verlag, Berlin Heidelberg New York, pp 491–537

Kilburn CR (2000) Lava flows and flow fields. In: Sigurdsson H (ed) Encyclopedia of volcanoes. Academic Press, San Diego, pp 291–306

Kilburn CRJ (2004) Fracturing as a quantitative indicator of lava flow dynamics. J Volcanol Geotherm Res 132:209–224

Lipman PW, Banks NG (1987) Aa flow dynamics, Mauna Loa 1984. US Geol Surv Prof Pap 1350:1527–1567

Lyman AW, Koenig E, Fink JH (2004) Predicting yield strengths and effusion rates of lava domes from morphology and underlying topography. J Volcanol Geotherm Res 129:125–138

Macdonald GA (1953) Pahoehoe, aa, and block lava. Am J Sci 251:169–191

Mazzarini F, Pareschi MT, Favalli M, Isola I, Tarquini S, Boschi E (2005) Morphology of basaltic lava channels during the Mt. Etna September 2004 eruption from airborne laser altimeter data. Geophys Res Lett 32: doi:10.1029/2004GL021815

Moore HJ (1987) Preliminary estimates of the rheological properties of 1984 Mauna Loa lava. US Geol Surv Prof Pap 1350:1569–1588

Neri A (1998) A local heat transfer analysis of lava cooling in the atmosphere: Application to thermal diffusion-dominated lava flows. J Volcanol Geotherm Res 81:215–243

Peterson DW, Holcomb RT, Tilling RI, Christiansen RL (1994) Development of lava tubes in the light of observations at Mauna Ulu, Kilauea Volcano, Hawaii. Bull Volcanol 56:343–360

Pinkerton H, Sparks RSJ (1978) Field measurements of the rheology of flowing lava. Nature 276:383–385

Pinkerton H, Wilson L (1994) Factors controlling the lengths of channel-fed lava flows. Bull Volcanol 56:108–120

Pinkerton H, Norton G (1995) Rheological properties of basaltic lavas at sub-liquidus temperatures: Laboratory and field measurements on lavas from Mount Etna. J Volcanol Geotherm Res 68:307–323

Pinkerton H, James M, Jones A (2002) Surface temperature measurements of active lava flows on Kilauea Volcano, Hawai`i. J Volcanol Geotherm Res 113:159–176

Pompilio M, Triglia R, Zanon V (1998) Melting experiments on Mt. Etna lavas; I, The calibration of an empirical geothermometer to estimate the eruptive temperature. Acta Vulcanol 10:67–75

Rowland SK, Walker GPL (1990). Pahoehoe and aa in Hawaii: Volumetric flow rate controls the lava structure. Bull Volcanol 52:631–641

Sakimoto SEH, Zuber MT (1998) Flow and convective cooling in lava tubes. J Geophys Res 103:27465–27487

Sakimoto SHE, Gregg TKP (2001) Channeled flow: Analytic solutions, laboratory experiments, and applications to lava flows. J Geophys Res 106:8629–8644

Soule SA, Cashman KV (2004) The mechanical properties of solidified polyethylene glycol 600, an analog for lava crust. J Volcanol Geotherm Res 129:139–153

Soule SA, Fornari DJ, Perfit MR, Tivey MA, Ridley WI, Schouten H (2005) Channelized lava flows at the East Pacific Rise crest 9–10°N: the importance of off-axis lava transport in developing the architecture of young oceanic crust. Geochem Geophys Geosyst 6, Q08005, doi:10.1029/2005GC000912

Tallarico A, Dragoni M (1999) Viscous Newtonian laminar flow in a rectangular channel: Application to Etna lava flows. Bull Volcanol 61:40–47

Tallarico A, Dragoni M (2000) A three-dimensional Bingham model for channeled lava flows. J Geophys Res 105:25969–25980

Tilling RI, Christiansen RL, Duffield WA, Endo ET, Holcomb RT, Koyanagi RY, Peterson DW, Unger JD (1987) The 1972–1974 Mauna Ulu eruption, Kilauea Volcano: An example of quasi-steady-state magma transfer. US Geol Surv Prof Pap 1350:405–469

Wolfe EW (ed) (1988) The Puu Oo eruption of Kilauea Volcano, Hawaii: Episodes 1 through 20, January 3, 1983, through June 8, 1984. US Geol Surv Prof Pap 1463:1–251